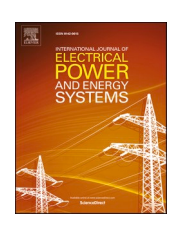
FISEVIER

Contents lists available at ScienceDirect

International Journal of Electrical Power and Energy Systems

journal homepage: www.elsevier.com/locate/ijepes





An optimal transmission line switching and bus splitting heuristic incorporating AC and N-1 contingency constraints[☆]

Majid Heidarifar *, Panagiotis Andrianesis, Pablo Ruiz, Michael C. Caramanis, Ioannis Ch. Paschalidis

Division of Systems Engineering, Boston University, Boston, MA, United States

ARTICLE INFO

Keywords:
Optimal transmission line switching
Bus splitting
Node-breaker modeling
AC optimal power flow
Mixed integer second order cone programming

ABSTRACT

Optimal transmission line switching and/or bus splitting is shown to contribute in relieving congestion and reducing the operation cost by rerouting power flows throughout the network. Although bus splitting may be as powerful as line switching in congestion mitigation and is typically considered a smaller disturbance compared with line switching, it has received less attention in the literature in part due to the more complicated node-breaker modeling requirement. In this paper, an optimal transmission line switching and bus splitting heuristic is presented to minimize the operation cost while respecting AC and N-1 contingency constraints. We present a two-level solution method where switching decisions are made in the upper level problem formulated as a mixed integer second order cone programming master problem, while the resulting network topology is checked against AC and N-1 contingency constraints in lower level subproblems. Line switching and bus splitting are modeled as switching actions assuming double-bus double-breaker substation arrangements where all elements at a substation, including generators, loads, lines and shunt elements, are given switches to connect to either of the busbars if the respective substation is split. We also introduce additional constraints to model a breaker-and-a-half substation scheme. Furthermore, a pre-screening step is presented to limit the search space of the problem, thus accelerating the solution process. We demonstrate the application of the proposed method on IEEE standard test systems.

1. Introduction

Optimal transmission line switching is the problem of co-optimizing the on/off status of transmission lines with the output of generators in power systems operation to relieve network congestion by rerouting power flows, thus decreasing the total operation cost. It is formulated as a Mixed Integer Linear Programming (MILP) problem in [1], incorporating Direct Current (DC) power flow equations and utilizing binary variables to represent switching status of transmission lines. To deal with the high combinatorial nature of the optimal transmission line switching problem, several pre-screening methods have been proposed to identify switching candidates [2–7]. In [8,9], optimal transmission line switching is accelerated by employing a reformulation of the problem using shift factors and flow cancelling transactions.

In addition to reducing the operation cost, the literature considers line switching as a flexibility resource to cope with the uncertainties caused by renewable energy resources; see, e.g., [10–13] in the context of power system operation and planning, respectively. Furthermore, line switching was employed to maximize power system load margin [14], to integrate into a stochastic joint energy and reserve market model [15], to suppress inter-area oscillation [16], to develop a controlled system splitting strategy [17], and to incorporate into a unit commitment model with short circuit current constraints [18]. Another application of transmission line switching is as a corrective action to enhance the system reliability by reducing post-contingency voltage and line flow violations [19]. Corrective transmission switching heuristics for large-scale real power systems are provided in [20,21].

However, line switching is not the only means of altering the topology; bus splitting is another switching action that enables a substation, i.e., a bus, to split to two or more separate busbars. Henceforth, a switching action implies line switching or bus splitting with both requiring switching circuit breakers within substations. Although bus splitting is typically considered a smaller disturbance compared with

E-mail addresses: mheidari@bu.edu (M. Heidarifar), panosa@bu.edu (P. Andrianesis), paruiz@bu.edu (P. Ruiz), mcaraman@bu.edu (M.C. Caramanis), yannisp@bu.edu (I.Ch. Paschalidis).

^{*} Research partially supported by NSF AiTF 1733827.

^{*} Corresponding author.

Nomenclature			Total shunt susceptance of line k .
Indices		$egin{array}{c} c_g \ M \end{array}$	cost coefficient of generator g.
d	Index for loads.		Big <i>M</i> . Number of generators.
u e	Index for each side of a line: $e \in \{F, T\}$.	n_g	
	Index for each side of a line, $e \in \{r, 1\}$. Index for generators.	p_d	Real power demand of load d.
g h	Index for shunt elements (capacitors, reactors).	q_d	Reactive power demand of load <i>d</i> . Series resistance and reactance of line <i>k</i> .
i i	Index for busses (substations).	r_k, x_k	series resistance and reactance of fine k.
i i	Index for busbars in a substation: $j \in \{1,2\}$.	Variables	
j k	Index for transmission lines.	I_k	Complex current flow of line <i>k</i> .
K.	muck for transmission mics.	$l_{k,j}^e$	Squared current magnitude of line k at the end side e
Sets		K.J	through busbar j.
\mathscr{D}_i	Set of loads connected to bus i.	l_k	Squared current magnitude of line k .
$\mathscr{G}_{\mathfrak{i}}$	Set of generators connected to bus <i>i</i> .	$p_{k,j}^e,q_{k,j}^e$	Real and reactive power flow of line k at the end side e
$\mathcal{H}_{\mathbf{i}}$	Set of shunt elements connected to bus <i>i</i> .	$P_{k,j}, q_{k,j}$	through busbar j.
${\mathscr I}$	Set of busses.	n a	Real and reactive demand of load d at busbar j of the
\mathscr{L}^F_i	Set of lines connected to bus <i>i</i> at the <i>from</i> end.	$p_{d,j},q_{d,j}$	
\mathscr{L}_{i}^{T}	Set of lines connected to bus <i>i</i> at the <i>to</i> end.	n a	corresponding substation. Real and reactive generation of generator <i>g</i> at busbar <i>j</i> of
$\mathscr{L}_{\mathbf{i}}$	Set of lines connected to bus <i>i</i> .	$p_{g,j},q_{g,j}$	the corresponding substation.
		n a	Real and reactive generation of generator <i>g</i> .
Paramete		p_g, q_g	Real and reactive generation of generator g .
α	Maximum allowed number of switching actions (both line	p_k, q_k	
	switching and bus splitting).	q_k^h	Shunt reactive power injection at each end of line <i>k</i> .
eta, γ	Maximum allowed number of line switching and bus	$ u_k^e, \delta_l^e$	Voltage squared magnitude and phase angle at the end side
	splitting actions, respectively.		e of line l.
$\overline{s}_k, \overline{l}_k$	Upper limits on apparent power and squared current flow	$v_{i,j}, \delta_{i,j}$	Voltage squared magnitude and phase angle at busbar <i>j</i> of
	of line <i>k</i> , respectively.		bus i, respectively.
$\underline{\delta}, \overline{\delta}$	Lower and upper limits on voltage phase angles.	V_{i}	Complex voltage variable at bus <i>i</i> .
$\underline{p}_{g},\overline{p}_{g}$	Lower and upper limits on real power generation of	$y_g, y_d, y_h,$	
-g - s	generator g.		j of the corresponding substation (0: $j = 1, 1$: $j = 2$).
$\underline{q}_{g},\overline{q}_{g}$	Lower and upper limits on reactive power generation of	z_i	Binary variable representing the state of bus <i>i</i> (1: connected
_ 8 0	generator g.		busbars, 0: split busbars
$\underline{v}, \overline{v}$	Lower and upper limits on voltage squared magnitude.	z_k	Binary variable representing the state of line k (1: in
a_k	Ideal transformer tap ratio in line k model.		service, 0: out of service).
B_h	Total susceptance of shunt element <i>h</i> .		

line switching, it has received less attention in the literature in part due to the more complex node-breaker modeling requirement. The authors in [7,22–28] utilize bus splitting to improve power system operation. [7] illustrates a better performance of bus splitting, compared with line switching, on the IEEE-118 test system; splitting two substations was shown to yield more cost savings compared with an unlimited number of line switching actions. [27] employs the shift factor methodology of [8] to model the breakers within a substation and presents two different formulations to find the optimal network topology.

Apart from improving the system operational efficiency, line switching and bus splitting has been shown to contribute in relieving overloads and voltage violations caused by contingencies [26]. The line switching and bus splitting model of [7] was shown to enhance power system reliability [29,30], and resilience under windstorms [31] and cyber-physical attacks [32]. The same model was further employed to show the capability in relieving the congestion and stress caused by plug-in hybrid electric vehicles [33], and in reducing wind power curtailment when combined with dynamic line rating [34]. Better performance of the line switching and bus splitting model of [7] compared with line switching only model was observed in [30,34] in terms of reducing the operation cost.

Although a DC power flow model is commonly employed in the literature, (e.g., in [1,3–5,7,8,27]), it may well happen that the switching actions violate the physics of the system governed by Alternating Current (AC) feasibility or undesirably increase the operation cost. In addition, DC-based methodologies are unable to relieve voltage congestion. In this respect, optimal transmission line switching is

evaluated with AC power flow constraints in [35-40]. [35] presents a Benders decomposition algorithm in which line switching decisions are made in the master problem and AC feasibility check is performed in the subproblems. This approach falls short in removing voltage congestion as voltage variables are not present in the master problem. [36] demonstrates the shortcomings of applying the DC-based pre-screening method in [5] to AC power flows and improves its performance. [37] proposes a heuristic algorithm that involves iteratively solving several AC Optimal Power Flow (OPF) cases. [38] employs a semidefinite programming relaxation to provide lower bounds for single line switching cases. [39] also uses a convex relaxation, but neglects line shunt susceptances and transformer tap ratios. [40] presents a strengthened convex relaxation formulation with three types of valid inequalities. A first attempt to solve the bus splitting problem with AC constraints is made in [41], which does not consider line switching and employs a substation model involving only transmission lines, without considering generators, loads, and transformers. N-1 contingency analysis in [27,42,43] uses DC power flow constraints, while the AC-based approach in [35] does not include bus splitting.

In this paper, we consider optimal transmission line switching and bus splitting problem, including both AC power flow constraints and N-1 contingencies to reduce the operation cost. First, we present a substation model with both line switching and bus splitting capabilities, which applies to two widely used substation schemes, namely the double-bus double-breaker and the breaker-and-a-half arrangements. Second, we propose a heuristic method which is based on (i) a pre-screening step to identify candidate substations, which significantly reduces the

computation effort by reducing the number of binary variables, and (ii) a two-level solution method in which the upper level is a master problem formulated as a Mixed Integer Second Order Cone Programming (MISOCP) problem aiming at identifying line switching and bus splitting actions subject to a convex approximation of power flow equations, whereas at the lower level the solution is evaluated for AC feasibility and N-1 contingency compliance. Third, we demonstrate the effectiveness of the proposed method by obtaining numerical solutions for several IEEE standard test systems.

The remainder of this paper is structured as follows: Section 2 presents the substation model with line switching/bus splitting capabilities. Section 3 describes the proposed heuristic method, and Section 4 provides and discusses the numerical results. Section 5 summarizes the main findings.

2. Transmission line switching and bus splitting model

In this section, we present the formulation of the transmission line switching and bus splitting model. In Section 2.1, we provide a convex approximation of the power flow equations, which are employed in our model. The detailed formulation is presented in Section 2.2.

2.1. Power flow model

Following [44] the AC power flow equations can be written as:

$$\sum_{g \in \mathcal{G}_i} p_g - \sum_{d \in \mathcal{D}_i} p_d - \sum_{k \in \mathcal{L}_i^F} p_k + \sum_{k \in \mathcal{L}_i^T} (p_k - r_k l_k) = 0, \ \forall i,$$
 (1)

$$\sum_{g \in \mathscr{T}_i} q_g - \sum_{d \in \mathscr{T}_i} q_d - \sum_{k \in \mathscr{T}_i^F} \left(q_k - q_k^h \right) + \sum_{h \in \mathscr{T}_i} q_h$$

$$+ \sum_{k \in \mathscr{T}_i^F} \left(q_k^h + q_k - x_k l_k \right) = 0, \quad \forall i,$$
(2)

$$p_k + \mathbf{j}q_k = V_k^F I_k^*, \ \forall k, \tag{3}$$

$$V_k^F/a_k - V_k^T = a_k(r_k + \mathbf{j}x_k)I_k, \ \forall k,$$

$$\tag{4}$$

where $j=\sqrt{-1}, l_k=|I_k|^2$ the squared magnitude of the complex line current flow I_k , and V_k^T and V_k^T the complex voltage variables at from and to end busses, respectively. Consider shunt element h and line k connected to bus i whose shunt reactive power injections are given by $q_h=B_hv_i$ and $q_k^h=B_kv_i/2$, respectively, where v_i is the voltage squared magnitude at bus i. (1) and (2) are the real and reactive power balance equations at bus i. (3) describes the nonlinear relation between power, current and from end voltage of line k, while (4) is the voltage drop across line k.

The nonlinear AC power flow Eqs. (1)–(4) appear as equality constraints in an ACOPF problem, thus yielding a nonconvex optimization problem. Several convex relaxation schemes have been proposed in the literature. Among them the second-order cone programming (SOCP) is the simplest computationally. The SOCP relaxation replaces (3) and (4) with (5) and (6) below and removes the voltage phase angle variables throughout the process, which often yields an inexact solution for a meshed transmission network [45]. To improve the SOCP relaxation, we add (7) that involves voltage phase angle variables (see [39] for more details):

$$l_k v_k^F - \left(p_k^2 + q_k^2\right) \geqslant 0, \ \forall k, \tag{5}$$

$$v_k^T - v_k^F / a_k^2 + 2(r_k p_k + x_k q_k) - a_k^2 (r_k^2 + x_k^2) l_k = 0, \forall k,$$
(6)

$$\delta_k^F - \delta_k^T = x_k p_k - r_k q_k, \ \forall k. \tag{7}$$

We present next a substation model that enables both line switching and bus splitting. We incorporate the convex approximation of OPF and provide the problem constraints.

2.2. A line switching and bus splitting model

2.2.1. Node-breaker models

A high-voltage substation is a junction point where system components, such as generators, transformers, lines, loads, etc., are connected in a special arrangement of circuit breakers and busbars. In this paper, we focus on two of the most widely used schemes, namely the doublebus double-breaker and the breaker-and-a-half arrangements shown in Fig. 1-a and -b, -a and -b, respectively. While the former provides higher reliability at the expense of higher cost by requiring two breakers per circuit, the latter is typically the recommended scheme for high voltage transmission substations (e.g., ISO-NE [46]) as it needs one-and-a-half breakers per circuit. Because of the complexities in modeling substation arrangements, steady-state power system analysis that includes optimal transmission line switching typically employs simple busbranch models, where the substation is represented with a single bus per voltage level. Utilizing a complete substation model, known as a node-breaker model in the literature, however, provides a higher degree of flexibility, allowing the splitting of a substation to two or more separate busbars.

Node-breaker models presented in [24–26,41] employ zero impedance lines (ZILs) — e.g., [26] introduces a new node for every network component connected to a substation and defines a ZIL between every node within that substation. Such models significantly increase the number of nodes, the dimension of the admittance matrix, and the number of binary variables. [7] presents a less computationally demanding substation model, employing only a single ZIL to allow for bus splitting. In the next subsection, we extend the model in [7] to incorporate AC power flow constraints.

2.2.2. Proposed substation model

Fig. 2 shows the proposed substation model where two busses i and i' are connected through transmission line k consisting of an ideal transformer in series with a Π model. Binary variable z_k is used to represent the on/off status of transmission line k. Without loss of generality, consider substation i in Fig. 2 where it can be split to two separate busbars using the binary variable z_i where $z_i=0$ indicates that the substation is split. All the elements within this substation, including lines, generators, loads and shunt elements can connect to either of the busbars through their respective binary variables y, with y=0 indicating connection to Busbar 1, and y=1 indicating connection to Busbar 2. Bus splitting scenarios of the double-bus double-breaker and the breaker-and-a-half arrangements of Fig. 1 can be equivalently modeled using the proposed substation model of Fig. 2. For example, opening CB1, CB4, and CB6 in double-bus double-breaker arrangement of Fig. 1-a is equivalently modeled with $z_i=0$, $y_{k1}^F=1$, $y_{k3}^T=0$, $y_{d1}=0$.

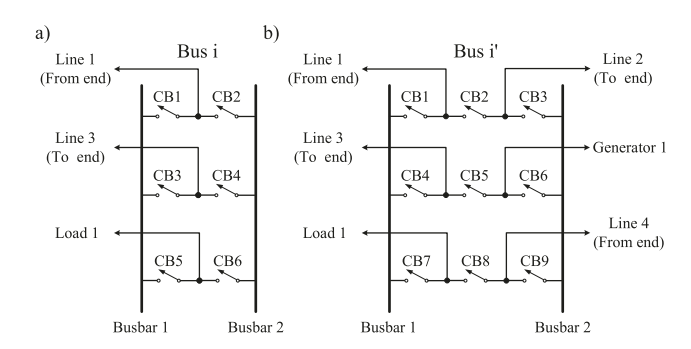


Fig. 1. (a) Double-bus double-breaker arrangement. (b) Breaker-and-a-half arrangement.

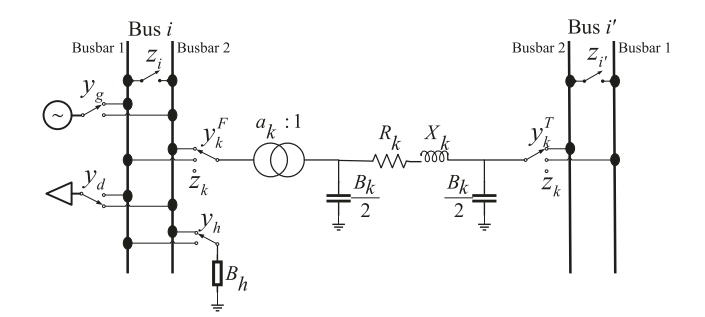


Fig. 2. Proposed Line Switching/Bus Splitting model.

As another example, the bus splitting event resulting from opening CB1, CB5, and CB8 in the breaker-and-a-half scheme (Fig. 1-b) is equivalent to setting $z_{\tilde{l}}=0,y_{k1}^F=1,y_{k3}^T=0,y_{d1}=0,y_{k2}^T=1,y_{g1}=1,y_{k4}^F=1$ in Fig. 2.

The proposed model is capable of representing all possible switching actions in double-bus double-breaker arrangement except for the disconnection of loads, generators and shunt elements, which, however, is not within the scope of this paper. The proposed model allows bus splitting while giving all equipment the capability to independently select which busbar to connect to, thus providing the flexibility of the double-bus double-breaker arrangement. Note that the breaker-and-ahalf scheme is comparatively less flexible, thus requiring additional constraints to accurately represent feasible bus splitting scenarios. An example of infeasible bus splitting scenario in the breaker-and-a-half scheme of Fig. 1-b is to connect Line 2 and Line 3 to Busbar 2 while Line 1 and Generator 1 are connected to Busbar 1 regardless of the connection status of Line 4 and Load 1. Overall, connection of two circuits on different bays and opposing sides, e.g., Line 2 and Line 3, to the same busbar is not possible if the other two circuits, e.g., Line 1 and Generator 1, are connected to the other busbar. This is expressed as:

$$-1 \leq (y_{k_1}^F + y_{g_1}) - (y_{k_2}^T + y_{k_3}^T) \leq 1, \tag{8}$$

which removes the possibility of both y variables in one parenthesis being 1, while the y variables in the other parenthesis are both 0. Similar constraints associated with the first/third and second/third bays guarantee removing other infeasible bus splitting scenarios. In addition, for constraints of the form (8) to accurately model bus splitting flexibility in breaker-and-a-half arrangement, we require a single switching action (line switching or bus splitting) at a time.

2.2.3. Model constraints

In what follows, we present the substation model shown in Fig. 2. As pointed out previously, we employ binary variable z_i to allow bus splitting, expressed as:

$$-M_i^{\delta}(1-z_i) \leqslant (\delta_{i,1}-\delta_{i,2}) \leqslant M_i^{\delta}(1-z_i), \ \forall i,$$

$$\tag{9a}$$

$$-M_i^{\nu}(1-z_i) \leqslant (\nu_{i,1}-\nu_{i,2}) \leqslant M_i^{\nu}(1-z_i), \ \forall i,$$
(9b)

which ensures equal voltage phase angles/squared magnitudes at both busbars if substation i is not split ($z_i = 1$). Consider generator g at substation i which can be connected to either of the busbars using the following constraints:

$$(1 - y_g)\underline{p}_{\sigma} \leqslant p_{g,1} \leqslant (1 - y_g)\overline{p}_g, \ \forall g \in \mathcal{G}_i, \tag{10a}$$

$$(1 - y_g)q_g \leqslant q_{g,1} \leqslant (1 - y_g)\overline{q}_g, \ \forall g \in \mathcal{G}_i, \tag{10b}$$

$$y_{g}\underline{p}_{g} \leqslant p_{g,2} \leqslant y_{g}\overline{p}_{g}, \ \forall g \in \mathcal{G}_{i},$$
 (10c)

$$y_g q_{\sigma} \leqslant q_{g,2} \leqslant y_g \overline{q}_g, \ \forall g \in \mathcal{G}_i,$$
 (10d)

where $y_g=0$ and $y_g=1$ indicate a connection of generator g to Busbar 1 and Busbar 2, respectively. Similar constraints are applied to Load d as follows:

$$p_{d,1} = (1 - y_d)p_d, \ q_{d,1} = (1 - y_d)q_d, \ \forall d \in \mathcal{D}_i,$$
 (11a)

$$p_{d,2} = y_d p_d, \ q_{d,2} = y_d q_d, \ \forall d \in \mathcal{D}_i. \tag{11b}$$

The reactive power injected/consumed by the shunt capacitor/reactor h at substation i would be $B_h v_{i,j}$ if there is a connection to Busbar j, and zero otherwise, which are represented by the following set of constraints:

$$-y_h M_h \leqslant q_{h,1} - B_h v_{i,1} \leqslant y_h M_h, \ \forall h \in \mathcal{H}_i, \tag{12a}$$

$$-(1-y_h)M_h \leqslant q_{h,2} - B_h v_{i,2} \leqslant (1-y_h)M_h, \forall h \in \mathcal{H}_i, \tag{12b}$$

$$-(1-y_h)M_h \leqslant q_{h,1} \leqslant (1-y_h)M_h, \ \forall h \in \mathcal{H}_i, \tag{12c}$$

$$-y_h M_h \leqslant q_{h,2} \leqslant y_h M_h, \ \forall h \in \mathcal{H}_i. \tag{12d}$$

In addition, transmission lines can be connected to either of the busbars at each end, i.e., *from* and *to*, or be switched off. Constraints (13a) and (13b) ensure that if Line k is not directly connected to Busbar j at end side e, power/current flow variables $p_{k,j}^e, q_{k,j}^e$ and $l_{k,j}^e$ would be zero, while (13c) imposes zero power/current flow along line k if the line is switched off. (13d) describes the power/current flow along line k considering the respective variables at the two ends.

$$\left(p_{k,1}^{e}\right)^{2} + \left(q_{k,1}^{e}\right)^{2} \leq \left(1 - y_{k}^{e}\right)\overline{s}_{k}^{2}, \ l_{k,1}^{e} \leq \left(1 - y_{k}^{e}\right)\overline{l}_{k}, \ \forall k, e,$$
 (13a)

$$\left(p_{k,2}^e \right)^2 + \left(q_{k,2}^e \right)^2 \le y_k^e \bar{s}_k^2, \ l_{k,2}^e \le y_l^e \bar{l}_k, \ \forall k, e,$$
 (13b)

$$\left(p_{k,1}^e \right)^2 + \left(q_{k,1}^e \right)^2 \le z_k \overline{s}_k^2, \ l_{k,1}^e \le z_k \overline{l}_k, \ z_k - y_k^e \ge 0, \forall k, e,$$
 (13c)

$$p_k = p_{k,1}^e + p_{k,2}^e, \ q_k = q_{k,1}^e + q_{k,2}^e, \ l_k = l_{k,1}^e + l_{k,2}^e, \ \forall k, e.$$
 (13d)

We define voltage squared magnitude and phase angle variables at each end of line k and enforce constraints (14a)–(14d) to ensure proper association of the aforementioned line variables with those of the busbars.

$$-y_{k}^{e}M_{k}^{\delta} \leq (\delta_{k}^{e} - \delta_{i,1}) \leq y_{k}^{e}M_{k}^{\delta}, \ \forall k \in \mathcal{L}_{i}, e, \tag{14a}$$

$$-(1-y_k^e)M_k^\delta \leqslant (\delta_k^e - \delta_{i,2}) \leqslant (1-y_k^e)M_k^\delta, \ \forall k \in \mathcal{L}_i, e, \tag{14b}$$

$$-y_k^e M_k^v \le (v_k^e - v_{i,1}) \le y_k^e M_k^v, \ \forall k \in \mathcal{L}_i, e, \tag{14c}$$

$$-\left(1-y_{k}^{e}\right)M_{k}^{v}\leqslant\left(v_{k}^{e}-v_{i,2}\right)\leqslant\left(1-y_{k}^{e}\right)M_{k}^{v},\ \forall k\in\mathscr{L}_{i},e.\tag{14d}$$

We add a modified version of power flow constraints (6) and (7) that takes the line on/off status variable z_k into account in (15a) and (15b), where $\zeta_k = 2(r_k p_k + x_k q_k) - a_k^2 (r_k^2 + x_k^2) l_k$ and $\eta_k = -(x_k p_k - r_k q_k)$.

$$-M_{k}^{v}(1-z_{k}) \leq v_{k}^{T} - v_{k}^{F}/a_{k}^{2} + \zeta_{k} \leq M_{k}^{v}(1-z_{k}), \ \forall k,$$
(15a)

$$-M_k^{\delta}(1-z_k) \leqslant \delta_k^F - \delta_k^T + \eta_k \leqslant M_k^{\delta}(1-z_k), \ \forall k.$$
 (15b)

The line charging reactive power injection is modeled in (16a)–(16 g). As for the *from* side constraints (16a) and (16b), the line charging reactive power injection is given by $B_k v_{i,j}^F/(2a_k^2)$ if there is a connection to busbar j, where a_k is the tap ratio of the ideal transformer in the line model. The line charging reactive power injection at the to side is similarly given by $B_k v_{i,j}^F/(2)$ in (16c) and (16d). Finally, if there is no connection to busbar j (16e) and (16f) or the line is out of service (16g), we enforce a zero line charging reactive power injection.

$$-y_k^F M_k^h \leqslant q_{k,1}^h - B_k v_{i,1}^F / \left(2a_k^2\right) \leqslant y_k^F M_k^h, \ \forall k \in \mathcal{L}_i^F,$$

$$\tag{16a}$$

$$-\left(1-y_k^F\right)M_k^h \leqslant q_{k,2}^h - \frac{B_k v_{i,2}^F}{2a_k^2} \leqslant \left(1-y_k^F\right)M_k^h, \forall k \in \mathcal{L}_i^F, \tag{16b}$$

$$-y_k^T M_k^h \leqslant q_{k,1}^h - B_k v_{i,1}^T / 2 \leqslant y_k^T M_k^h, \ \forall k \in \mathcal{L}_i^T,$$

$$\tag{16c}$$

$$-\left(1-y_k^T\right)M_k^h \leqslant q_{k,2}^h - \frac{B_k v_{i,2}^T}{2} \leqslant \left(1-y_k^T\right)M_k^h, \forall k \in \mathcal{L}_i^T, \tag{16d}$$

$$-(1-y_k^e)M_k^h \leqslant q_{k,1}^h \leqslant (1-y_k^e)M_k^h, \ \forall k \in \mathcal{L}_i, e, \tag{16e}$$

$$-y_{\nu}^{e}M_{\nu}^{h} \leqslant q_{\nu}^{h} \lesssim y_{\nu}^{e}M_{\nu}^{h}, \ \forall k \in \mathcal{L}_{i}, e, \tag{16f}$$

$$-z_k M_k^h \leqslant q_{k,i}^h \leqslant z_k M_k^h, \ \forall k \in \mathcal{L}_i, j.$$
 (16g)

3. Proposed solution method

In this section, we present the proposed heuristic method to solve the optimal transmission line switching and bus splitting problem subject to AC and N-1 contingency constraints.

As shown in Fig. 3, the proposed heuristic method starts with a prescreening of network busses to identify candidate substations, which significantly decreases the computation effort by reducing the number of binary variables associated with switching decisions. The method follows a two-level solution strategy, in which the upper level is a master problem and the lower level includes two subproblems. The master problem, which aims to identify the switching actions, is formulated using the substation model presented in Section 2.2 as an MISOCP problem. SubProblem 1 is a Nonlinear Programming (NLP) problem, which checks whether (i) the topology obtained by the master problem is feasible, and (ii) the cost function has decreased compared with the base case, i.e., prior to applying the switching or splitting actions. If the conditions (i.e., AC feasibility and cost reduction) of SubProblem 1 are satisfied, SubProblem 2 is solved to evaluate compliance with N-1 contingency requirements. If either of the subproblems is infeasible or the cost function has increased, an integer cut is added to the master problem to remove the identified topology from the search space so that the algorithm does not identify the same invalid topology in the next iterations. Note that, following the common practice of operators to perform only one action at a time, we limit the number of switching

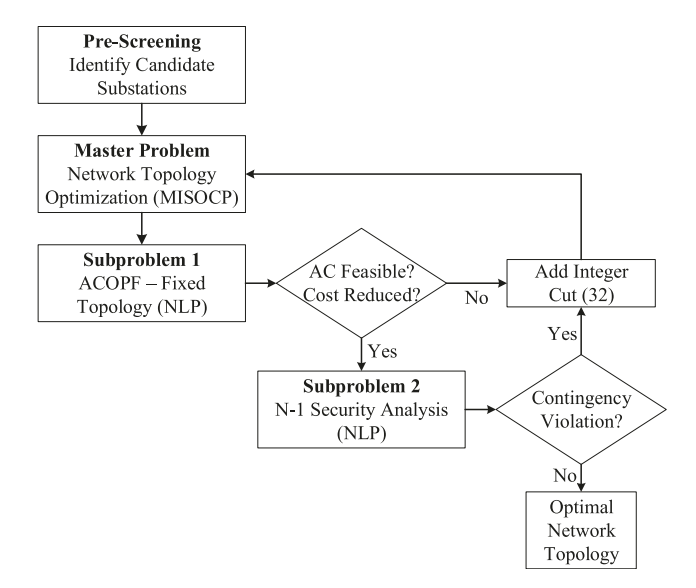


Fig. 3. Flowchart of the proposed heuristic method.

actions to 1, and iteratively apply the proposed method to derive a sequence of N-1 compliant and AC feasible actions.

In what follows, we present the pre-screening step in Section 3.1, the master problem formulation in Section 3.2, SubProblems 1 and 2 in Sections 3.3 and 3.4, respectively, and the integer cuts in Section 3.5.

3.1. Pre-screening step

Integrality constraints associated with switching actions create a hard combinatorial optimization problem for large scale power systems. Therefore, a pre-screening step to reduce the number of candidate substations/lines is very common — if not unavoidable — in practical applications [3,5,7]. In the context of DC power flow-based optimal transmission switching, [2,3,5,7] use sensitivity analysis to select candidate lines/substations. The study in [2,5] selects lines with counter-economic flows, i.e., lines that carry power from a higher Locational Marginal Price (LMP) bus to a lower one, while the analysis performed by [3] introduces three additional sensitivity criteria, which tend to select either the congested lines or those feeding or are being fed by these lines. Contrary to approaches presented in [2,3,5], which find candidate lines, [7] identifies candidate substations by clustering the system busses into congestion zones using LMPs. The boundary busses are then selected as the candidate substations.

Extending the work in [7] to the context of AC power flow, we present a pre-screening step, which uses real LMPs (P-LMPs) and reactive LMPs (Q-LMPs) to find candidate substations. Note that P-LMP and O-LMP at a bus are the dual variables associated with the real and reactive power balance constraints, respectively, which can be obtained by solving ACOPF on the base test system. The proposed pre-screening step involves the following: (i) Clustering busses into congestion zones using Fuzzy C-means algorithm, where P-LMPs and Q-LMPs are clustering features, and (ii) selecting boundary busses that have four or more connected lines as candidates for switching actions. Prior to applying the Fuzzy C-means algorithm, the number of clusters needs to be determined. The number of clusters depends on the level, location, and severity of congestion (binding voltage or line thermal limits), and it has certain implications to the computation times and the cost savings. A smaller number of clusters results in a smaller list of candidate substations, a smaller search space, and lower computation times. On the other hand, the potential cost savings are limited to those of the identified candidate substations.

3.2. The master problem

The master problem incorporates the substation model of Fig. 2 to identify a candidate topology. The proposed substation model, however, introduces a large number of binary variables for practical-sized power systems, thus creating a computationally complex Mixed Integer Programming (MIP) problem. Nevertheless, adding integer constraints is expected to improve the computational complexity of the problem as the optimal solution to the corresponding linear programming relaxation would be closer to the optimal solution of the MIP problem in a branch and cut algorithm [47]. In fact, it is widely known that limiting the number of line switching actions through an integer constraint reduces the computational effort [1].

Hence, we first add a constraint to limit the total number of switching actions, including both line switching and bus splitting, to a single action:

$$\sum_{k} \left(1 - z_k \right) + \sum_{i} \left(1 - z_i \right) \leqslant 1. \tag{17}$$

Notably, it is shown in several works, (e.g., [1,3,7]), that although limiting the number of switching actions may result in a sub-optimal solution, it usually captures most of the potential cost savings. Furthermore, multiple switching actions can be found by consecutively

solving for single switching actions.

To motivate the next set of integer constraints, consider a case where substation i is not split, i.e., $z_i = 1$. Altering the y variables at this substation cannot change the objective function value, therefore, fixing the y variables to zero shrinks the feasibility set:

$$z_i - 1 + y_g \leqslant 0, \ z_i - 1 + y_d \leqslant 0, \ \forall i, g \in \mathcal{G}_i, d \in \mathcal{D}_i,$$

$$\tag{18a}$$

$$z_i - 1 + y_h \leqslant 0, \ z_i - 1 + y_i^e \leqslant 0, \ \forall i, h \in \mathcal{H}_i, k \in \mathcal{L}_i.$$
 (18b)

The last set of integer constraints requires that at least two lines be connected to each busbar if the corresponding substation splits to maintain the system reliability:

$$\sum_{k \in \mathcal{I}_i} y_k^e \ge 2(1 - z_i), \ \sum_{k \in \mathcal{I}_i} (z_k - y_k^e) \ge 2(1 - z_i). \ \forall i.$$
 (19)

Note that as a result of applying constraint (19), substations with less than four connected lines would not be allowed to split. Except for that, it does not impose additional constraints on such substations.

We can now formulate the master problem as the following MISOCP problem:

$$\min \quad \sum_{g=1}^{N_G} c_g p_g, \tag{20}$$

subject to:
$$(5), (9) - (19)$$
 (21)

$$\sum_{g \in \mathscr{Y}_i} p_{g,j} - \sum_{d \in \mathscr{Y}_i} p_{d,j} - \sum_{k \in \mathscr{Y}_i^F} p_{k,j} + \sum_{k \in \mathscr{Y}_i^T} \left(p_{k,j} - r_k l_{k,j} \right) = 0, \forall i, j$$
 (22)

$$\sum_{g \in \mathscr{T}_i} q_{g,j} - \sum_{d \in \mathscr{T}_i} q_{d,j} - \sum_{k \in \mathscr{F}_i^F} \left(q_{k,j} - q_{k,j}^h \right) + \sum_{h \in \mathscr{F}_i} q_{h,j} + \sum_{k \in \mathscr{F}_i^T} \left(q_{k,j}^h + q_{k,j} - x_k l_{k,j} \right) = 0, \quad \forall i, j,$$
(23)

$$\underline{\delta}_{i,j} \leqslant \delta_{i,j} \leqslant \overline{\delta}_{i,j}, \ \underline{v}_{i,j} \leqslant \overline{v}_{i,j}, \ \forall i,j,$$
(24)

where the objective function is the minimization of the total real power generation cost. (22) and (23) are the real and reactive power balance equations at each busbar. (24) imposes operational limits on the voltage phase angle and squared magnitude variables. In addition, we add constraints of the form (8) for substations with breaker-and-a-half arrangement. After a new network topology is found by the master problem, we structure it in a bus-branch format and solve SubProblem 1 described below to check for AC feasibility and cost function reduction.

3.3. SubProblem 1

Since the master problem employs a convex approximation of the power flow equations, the network topology obtained by the master problem might be AC infeasible or it might undesirably increase the cost function value. Therefore, we apply an ACOPF to the topology obtained by the master problem to check for AC feasibility and cost reduction. Accordingly, SubProblem 1 is formulated as the following NLP problem:

minimize
$$(20)$$
 (25)

subject to:
$$(1) - (4), (24)$$
 (26)

$$p_k^2 + q_k^2 \leqslant \overline{s}_k, \ l_k \leqslant \overline{l}_k, \ \forall k, \tag{27}$$

$$\underline{p}_{g} \leqslant p_{g} \leqslant \overline{p}_{g}, \ \underline{q}_{g} \leqslant q_{g} \leqslant \overline{q}_{g}, \ \forall g.$$
 (28)

If SubProblem 1 is infeasible or if it increases the cost function compared

with the base case, i.e., prior to introducing reconfiguration, we remove the topology found by the master problem from the feasible space by adding certain cuts to the master problem. See Section 3.5 for more details.

3.4. SubProblem 2

If the topology found by the master problem satisfies the conditions of SubProblem 1, i.e., AC feasible and cost function reduction, it should be further evaluated for N-1 contingency constraints. In this paper, we define the N-1 contingency compliance as the capability of the system to withstand the loss of any single transmission element. Consider the contingency state c in which a single transmission line is lost. We formulate SubProblem 2 for state c as a feasibility problem with the following set of constraints:

$$(1) - (4), (24),$$
 (29)

$$p_{k,c}^2 + q_{k,c}^2 \leqslant \overline{s}_{k,c}, \ l_{k,c} \leqslant \overline{l}_{k,c}, \ \forall k, \tag{30}$$

$$p_{s} \leqslant p_{g,c} \leqslant \overline{p}_{g}, \ q_{s} \leqslant q_{g,c} \leqslant \overline{q}_{g}, \ \forall g, \tag{31}$$

where (1)–(4) enforce the AC power flow equations and (24), (30) and (31) the operational limits for contingency state *c*. A similar N-1 formulation with DC power flow equations can be found in [42]. If the network topology is feasible in all contingency states, then the optimal network topology is found, otherwise, we add integer cuts, presented in the next subsection, to remove the topology from the feasible space.

3.5. Integer cuts

If the network topology obtained by the master problem is shown to violate either of the subproblems, it is invalid and is removed from the search space. This can be done by adding (32) to the master problem:

$$\sum_{k \in \mathcal{X}} z_k + \sum_{h \in \mathcal{R}} z_b \geqslant 1,\tag{32}$$

where \mathcal{H} and \mathcal{B} are the set of open lines and split substations, respectively, in the topology identified by the master problem as invalid in the current iteration. Note that since we are restricting the search space in the proposed method, it may happen that the removed topology could have been valid had we followed a different search of actions. This is, however, common, to any heuristic method, which constrains the switching actions, for the sake of computational tractability.

4. Numerical results

In this section, we evaluate the performance of the proposed optimal transmission line switching and bus splitting heuristic method on three IEEE test systems, namely the IEEE-14, IEEE-57, and IEEE-118, with 14, 57, and 118 busses, respectively [48].

For all test systems, we adopt a breaker-and-a-half scheme for all reconfigurable substations and add constraints of the form (8) to limit the bus splitting flexibility. The data corresponding to generation capacity limits, generation cost functions, and branch thermal limits, which are missing in [48], are taken from the Power Grid Library for benchmarking the ACOPF problem, PGLib OPF [44]. The voltage squared upper and lower bounds are $\underline{v} = (0.94)^2$ and $\overline{v} = (1.06)^2$ p.u. for all test systems. Big M values are set at $M^v = \overline{v} - \underline{v}$, $M_k^h = B_k \overline{v} \mod (1.1)$

 a_k^2), $M_h = B_h \bar{\nu}$, and $M^{\delta} = \bar{\delta} - \underline{\delta}$, where $\bar{\delta} = -\underline{\delta} = \pi/6$ is the maximum allowed voltage phase angle. All simulations refer to a single hour, hence, the cost and LMP values are in \$/hr and \$/MWh, respectively.

To further evaluate the performance of the proposed method, we employ heavily loaded instances, called "Active Power Increase (API)"

test systems in PGLIB OPF. We denote the standard and heavily loaded test systems with "std" and "API", respectively. For example, 14-std and 14-API shall denote the IEEE-14 test system under standard and heavily loaded conditions, respectively. For all contingencies, we assume — as in [42] — that the emergency thermal limit is 125% of the steady state operating limit. We note that before conducting network reconfiguration, we evaluated the test systems for compliance with the N-1 contingency requirements. Aside from the radial transmission lines, which are not subject to N-1 criteria as defined by U.S. Federal Energy Regulatory Commission (FERC), we removed a few other lines from the contingency list whose loss could not be tolerated by the base test system. See Table 1 for a list of elements removed from the contingency list.

The proposed method is implemented in Matlab R2018a and tested on a laptop with Intel i7–8550U CPU at 1.80 GHz and 16 GB RAM. The master problem is modeled in YALMIP [49], A Toolbox for Modeling and Optimization in MATLAB, and solved using Gurobi, a commercially available solver. The ACOPF subproblems are solved using MAT-POWER's primal–dual interior point solver [50].

In Section 4.1, we evaluate the performance of the proposed heuristic method. In Section 4.2, we further discuss and elaborate on the prescreening step.

4.1. Performance of the proposed method

In this subsection, we evaluate the performance of the proposed method, in terms of cost savings and computation time.

We first consider the IEEE-14 test system. This is a small network which facilitates visualization. It includes 3 synchronous condensers and 2 generators, with generator located at Bus 1 being about 66% cheaper compared with the one located at Bus 2. Under std (API) loading conditions, the generation capacity is 154% (136%) of the load, and the base case total cost is \$2,178.1 (\$5,999.4), with 3 (3) binding voltage upper bound and no (2) congested lines. Pre-screening identifies 2 (3) congestion zones and the same 3 candidate busses, namely busses 2, 4 and 5. We visualize the pre-screening step in Fig. 4. In Fig. 4 (left), we depict a contouring of the 14-API test system using nodal P-LMPs ranging between \$7.92/MW and \$122.4/MW. Note that we ignored the contribution of Q-LMPs on the pre-screening step in 14-API test system as Q-LMPs were negligible compared with P-LMPs in this case. In Fig. 4 (right), we show the impact on P-LMP, after applying the bus splitting action on Bus 5, which is selected by the master problem. New P-LMPs now range from \$13.4/MW to \$43.77/MW. Note that a new bus, Bus 15, is added to the bus-branch representation of Fig. 4 (right) as a result of the bus splitting action. In addition to smoothing LMPs, the proposed bus splitting action relieves congestion in transmission line 2-3. However, the action on Bus 5 is finally rejected, as it violates N-1 constraints. Notably, all identified switching actions, which are capable of reducing the cost and are AC feasible, violate N-1 constraints.

Next, we consider the IEEE-57 test system. It includes 3 synchronous condensers and 4 generators whose marginal costs range between \$16.96/MW and \$37.19/MW. Under std (API) loading conditions, the generation capacity is 159% (141%) of the load, and the base case total cost is \$37,589.3 (\$49,296.7), with 3 (4) binding voltage constraints. Pre-screening identifies 9 (11) candidate busses, and we find a single switching action, namely Bus 4 (41), which results in cost savings of only

Table 1Transmission Branches Removed from N-1 Contingency List.

Test system	Non-Radial [Radial] Transmission Elements			
14-Std	1, [14]			
14-API	1, 3, 6, 10, 13, 17, [14]			
57-Std	22, 29, 35–43, 46–52, 55, 60–61, 65, 67, 79–80, [45]			
57-API	22, 29–30, 33, 35–44, 46–61,65–68, 71–72, 74, 76, 78–80, [45]			
118-Std	7, 133, 185, [9, 113, 134, 176–177, 183–184]			
118-API	7–8, 51–52, 104, 125, 133, 185, [9, 113, 134, 176–177, 183–184]			

about 0.007% (0.0003%), under the std (API) loading conditions, while meeting N-1 contingency requirements. The small cost savings are in part due to the absence of thermal line congestion in the base case.

The IEEE-118 test system has been extensively used in the literature for transmission line switching studies. It includes 35 synchronous condensers and 19 committed generators with marginal costs ranging from \$12.61/MW to \$124.58/MW. Under std (API) loading conditions, the generation capacity is 154% (137%) of the load, and the base case total cost is \$97,213.6 (\$242,054), with 2 (18) line thermal limit congestion and 11 (19) binding voltage constraints. Pre-screening clusters the network to 3 (4) zones, leading to the selection of 23 (30) candidate busses, i.e., a decrease in the number of candidates by 80% (74%), under the std (API) loading conditions. We find 5 consecutive switching actions, which include splitting busses 69, 103, 32, 77 and 59, (69, 17, 49, 30, and 94), with total cost savings of about 0.52%(19.91%), as depicted in Fig. 5 (left: std, right: API). As can be observed, most cost savings are obtained by the very first few switching actions under the std loading conditions. Notably, all identified switching actions are bus splitting, which further demonstrates its potential as a powerful switching action. Indeed, the potential cost savings depend on the network parameters and loading conditions. The significantly higher cost savings in the IEEE-118 test system compared with the 14-bus and 57-bus test systems are in part due to its wider range of generator marginal costs, where the highest cost generator is around 9 times more expensive than the lowest cost one, and in part due to the fact that, under the API loading conditions, the 118-bus test system is extremely

To demonstrate the relative performance of line switching compared with bus splitting, we applied the method allowing only for line switching actions (no bus splitting). We present the results of the comparison in Table 2. IEEE-14 and IEEE-57 test systems could not identify any AC-feasible and N-1 compliant line switching action. In the IEEE-118 test system, the cost savings after performing 5 line switching actions were 0.09% and 2.31%, under the std and API loading conditions, respectively, i.e., significantly lower compared with cost savings obtained when we allow for combined line switching and bus splitting.

We further evaluate the computational performance of the proposed method on the IEEE-118 test system. Fig. 6 depicts the total computation time with respect to the number of switching actions in a cumulative manner, where the first 5 switching actions are found in around 4.5 and 8.4 min, under std and API loading conditions, respectively. In addition to the total computation time, we illustrate separately the time spent on solving the master problem and the subproblems, which are the most time-consuming steps. The results indicate that under std loading conditions, the computation time of the master problem is slightly more than that of the subproblems, whereas under API loading conditions the solution time of the master problem dominates. The computation time required to run the pre-screening step on IEEE-118 test system is about 0.12 s, under both std and API loading conditions, which is negligible compared with the overall computation times reported in Fig. 6. We removed the pre-screening step, i.e., considered all substations with 4 or more connected lines as candidates, and observed that the total computation time was almost doubled under the std loading conditions, whereas no solution was obtained after 3 h under the API loading conditions. These results reiterate the importance of employing a prescreening step to reduce the number of binary variables and improve the overall computational performance and tractability of the line switching and bus splitting problem.

4.2. Pre-screening step evaluation and discussion

As already noted, the pre-screening step reduces the search space by narrowing the candidate substations/lines, hence, the resulting switching actions. Ideally, we would want the pre-screening step to identify candidates that have a high potential of cost savings; said differently, we would not want the pre-screening to discard candidate with a high

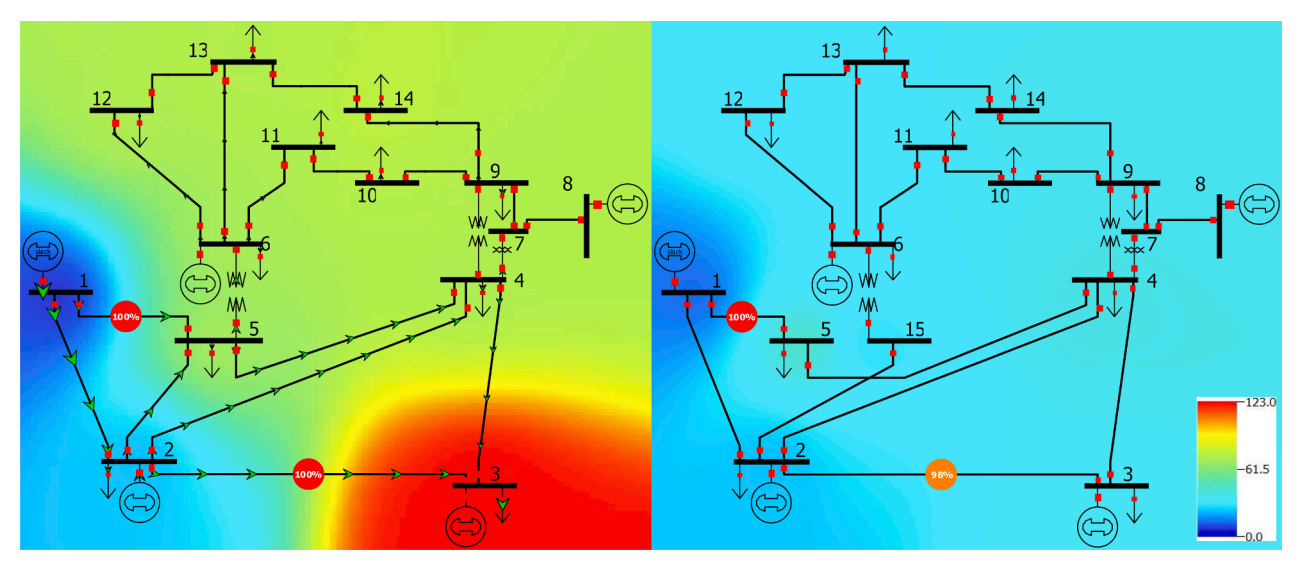


Fig. 4. Contouring of the IEEE-14 test system in API loading condition using P-LMPs. Left: before reconfiguration. Right: after reconfiguration (splitting Bus 5).

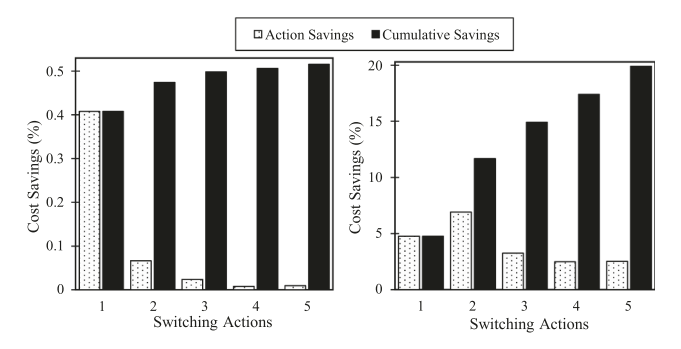


Fig. 5. Percent of cost savings vs. the number of switching actions in the IEEE-118 test system. All switching actions are bus splitting. (Left: std loading, Right: API loading).

Table 2Comparison of "Combined Line Switching and Bus Splitting" with "Only Line Switching."

Test system	Base Cost		Combined Line Switching and Bus Splitting		Only Line Switching	
		Cost Savings (%)	Switching Actions	Cost Savings (%)	Switching Actions	
14-Std	\$2,178.1	0%	None	0%	None	
14-API	\$5,999.4	0%	None	0%	None	
57-Std	\$37,589.3	0.007%	1B (4)	0%	None	
57-API	\$49,296.7	0.0003%	1B (41)	0%	None	
118-	\$97,213.6	0.52%	5B (69, 103,	0.09%	5L (166, 76,	
Std			32, 77, 59)		75, 57, 165)	
118- API	\$242,054	19.91%	5B (69, 17, 49, 30, 94)	2.31%	5L (150, 102, 165, 145, 39)	

potential of cost savings. In what follows, we calculate the potential cost savings obtained from applying only one single switching action, without performing the clustering and associated removal of non-boundary busses, i.e., in the absence of the pre-screening step. In other words, we exhaustively evaluate the potential cost savings associated with each feasible switching action. Equivalently, this can be thought of solving the master problem for each switching action, and then SubProblem 1 (AC OPF) to calculate the potential cost savings.

Since no switching action could satisfy N-1 contingency requirements for the IEEE-14 test system, we consider only the IEEE-57

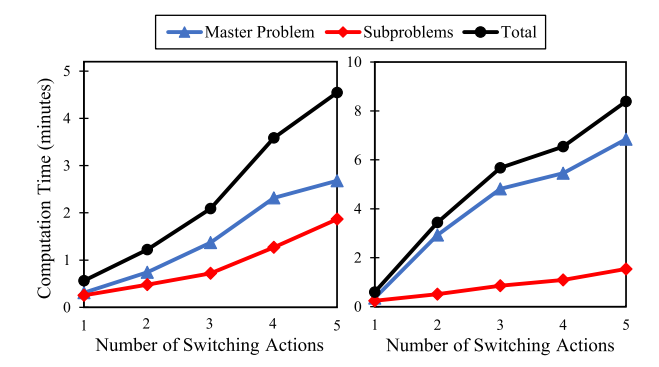


Fig. 6. Computation times in minutes for the IEEE-118 test system. All switching actions are bus splitting. (Left: std loading, Right: API loading).

and IEEE-118 test systems. The results of the cost savings are presented in Fig. 7 for both test systems (Fig. 7(a): IEEE-57, Fig. 7(b): IEEE-118). In each sub-Figure, we illustrate the results of the cost savings, under std (top) and API (bottom) loading conditions, and for line switching actions (left) and bus splitting actions (right), in four graphs. Blue diamonds represent the switching actions selected by the prescreening step (candidates). Red crosses represent the switching actions that were not selected (e.g., non-boundary busses). Both blue diamonds and red crosses represent AC-feasible switching actions. Recall that the resulting cost savings for each action are obtained by the solution of the ACOPF SubProblem 1. In addition, all switching actions that are N-1 compliant are circled.

Consider first the IEEE-57 test system (see Fig. 7(a)). Under std (API) loading conditions, Bus 24 (Line 13) prevails as the action with the highest potential cost savings of about 0.045% (0.016%). They are both included as candidates by the pre-screening; nevertheless, they are not eventually identified by the solution method since they both violate the N-1 contingency requirements. Note that there is only one AC-feasible switching action involving Line 62 that is not considered as candidate; this action, however, violates N-1 contingency requirements. In fact, in the IEEE-57 test system, there is only one action that is N-1 compliant, involving Bus 4 (Bus 41), which is indeed the selected one by the proposed method, under std (API) loading conditions (see also Table 2).

Consider next the IEEE-118 test system (see Fig. 7(b)). Note that the non-candidates, for both line switching and bus splitting actions, and under both std and API loading conditions, exhibit very low cost savings potential. In other words, the pre-screening performs well in identifying

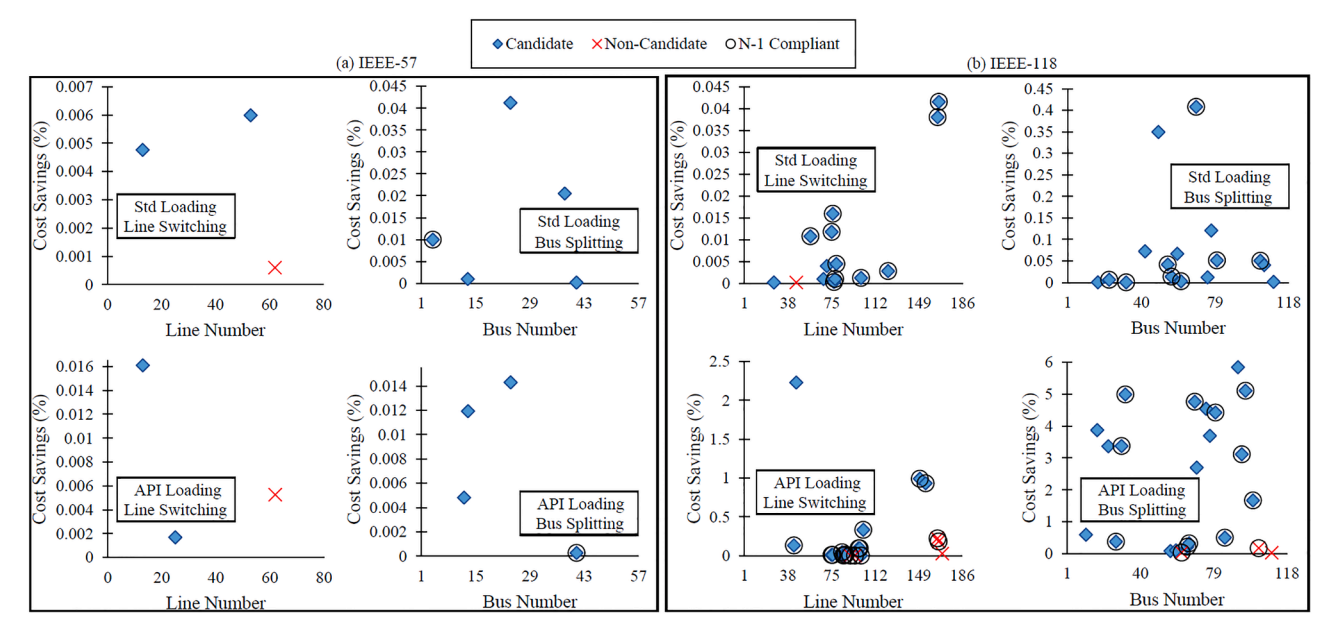


Fig. 7. Cost savings (in percent) for single switching actions in the IEEE-57 (a) and the IEEE-118 (b) test systems. In each sub-Figure, line switching (right) and bus splitting (left) actions are evaluated on std (top) and API (bottom) loading conditions.

candidates with a high cost savings potential. Under the std loading conditions, the action with the highest cost savings potential is to split Bus 69. Under the API loading conditions, the action with the highest cost savings potential is to split Bus 92; however, this action is not N-1 compliant, hence, it is not selected by the overall solution method. Evidently, in this test case, bus splitting actions result, in general, in higher cost savings.

Lastly, we evaluate the performance of the pre-screening step presented in [7], which employs DCOPF to find LMPs for clustering. Under both loading conditions of the IEEE-14 and IEEE-57 test systems, where congestion is mostly due to voltage limitations, the application of DCOPF could not observe congestion, thus being unable to find candidate busses/lines since LMPs are the same. DCOPF could not observe the line thermal congestion shown in the ACOPF simulation of the 14-API system in Fig. 4 (left) either; however, it showed transmission line 1–5 is 99% loaded, suggesting that it would have been congested, had we included losses and reactive power flow. In the IEEE-118 test system, however, the DCOPF-based pre-screening identified most, though not all, of the candidates found by its ACOPF-based counterpart. Employing the DCOPF-based pre-screening step without modifying the rest of the steps in the flowchart of Fig. 3 results, after 5 switching actions, in very similar cost savings to the ones reported in Section 4.1, namely 93.9% and 100% of the cost savings reported in Table 2 under std and API loading conditions, respectively. Therefore, one expects that a DCOPFbased pre-screening step to perform comparably to its ACOPF-based counterpart, when congestion is severe and mostly caused by binding line thermal limits.

5. Conclusions

In this paper, an optimal transmission line switching and bus splitting heuristic is proposed that includes AC and N-1 contingency constraints. The proposed method identifies a network topology that reduces the operation cost while maintaining AC feasibility and initial system reliability level in the sense of N-1 contingency requirements. Following an initial pre-screening to find candidate substations, a two-level solution method is employed in which the upper level is a master problem formulated as an MISOCP problem, which identifies line switching and bus splitting actions. The lower level checks for AC feasibility and N-1 contingency requirements. Simulation results on

several IEEE test systems demonstrate that (1) bus splitting is a powerful tool in relieving network congestion, (2) the potential cost savings depend highly on the operating (loading) conditions and network parameters, and (3) a DCOPF-based pre-screening step may occasionally fail to identify candidate busses/lines that relieve transmission line thermal congestion.

The proposed pre-screening step was demonstrated to play a major role in shrinking the feasible space and reducing the computation times on the IEEE test cases. Future research will focus on investigating the performance in large scale systems, as well as evaluating additional heuristics, e.g., selecting a single switching action from the list of candidates by evaluating a metric similar to the approach in [3] in the context of line switching. In addition to AC feasibility and N-1 requirements, additional aspects, which are also important in actual systems, such as transient and small-signal stability, will be further explored.

CRediT authorship contribution statement

Majid Heidarifar: Conceptualization, Methodology, Software, Formal analysis, Writing - original draft. Panagiotis Andrianesis: Methodology, Writing - review & editing. Pablo Ruiz: Validation, Writing - review & editing. Michael C. Caramanis: Supervision, Funding acquisition. Ioannis Ch. Paschalidis: Project administration.

Declaration of Competing Interest

The authors declare that they have no known competing financial interests or personal relationships that could have appeared to influence the work reported in this paper.

References

- Fisher EB, O'Neill RP, Ferris MC. Optimal transmission switching. IEEE Trans Power Syst Aug 2008;23(3):1346–55.
- [2] Ruiz PA, Foster JM, Rudkevich A, Caramanis MC. On fast transmission topology control heuristics. In: 2011 IEEE Power and Energy Society General Meeting; 2011.
- [3] Ruiz PA, Foster JM, Rudkevich A, Caramanis MC. Tractable transmission topology control using sensitivity analysis. IEEE Trans Power Syst 2012;27(3):1550–9.
- [4] Liu C, Wang J, Ostrowski J. Heuristic prescreening switchable branches in optimal transmission switching. IEEE Trans Power Syst 2012;27(4):2289–90.

- [5] Fuller JD, Ramasra R, Cha A. Fast heuristics for transmission-line switching. IEEE Trans Power Syst 2012;27(3):1377–86.
- [6] Goldis EA, Li X, Caramanis MC, Keshavamurthy B, Patel M, Rudkevich AM, Ruiz PA. Applicability of topology control algorithms (TCA) to a real-size power system. In: 2013 51st Annual Allerton Conference on Communication, Control, and Computing (Allerton); 2013. p. 1349–52.
- [7] Heidarifar M, Ghasemi H. A network topology optimization model based on substation and node-breaker modeling. IEEE Trans Power Syst Jan 2016;31(1): 247-55.
- [8] Ruiz PA, Rudkevich A, Caramanis MC, Goldis E, Ntakou E, Philbrick CR. Reduced MIP formulation for transmission topology control. In: 2012 50th Annual Allerton Conference on Communication, Control, and Computing (Allerton), Oct 2012b. p. 1073-1079
- [9] Ruiz PA, Goldis E, Rudkevich AM, Caramanis MC, Philbrick CR, Foster JM. Security-constrained transmission topology control MILP formulation using sensitivity factors. IEEE Trans Power Syst 2017;32(2):1597–605.
- [10] Taheri MH, Dehghan S, Heidarifar M, Ghasemi H. Adaptive robust optimal transmission switching considering the uncertainty of net nodal electricity demands. IEEE Syst J 2017;11(4):2872–81.
- [11] Aghaei J, Nikoobakht A, Mardaneh M, Shafie-khah M, Catalão JPS. Transmission switching, demand response and energy storage systems in an innovative integrated scheme for managing the uncertainty of wind power generation. Int J Electr Power Energy Syst 2018;98:72–84.
- [12] Nikoobakht A, Aghaei J, Niknam T, Farahmand H, Korpås M. Electric vehicle mobility and optimal grid reconfiguration as flexibility tools in wind integrated power systems. Int J Electr Power Energy Syst 2019;110:83–94.
- [13] Zhang H, Cheng H, Liu L, Zhang S, Zhou Q, Jiang L. Coordination of generation, transmission and reactive power sources expansion planning with high penetration of wind power. Int J Electrical Power Energy Syst 2019;108:191–203.
- [14] Haghighat H. Loading margin calculation with line switching: A decomposition method. Int J Electrical Power Energy Syst 2015;64:104–11.
- [15] Aazami R, Haghifam MR, Soltanian F, Moradkhani M. A comprehensive strategy for transmission switching action in simultaneous clearing of energy and spinning reserve markets. Int J Electrical Power Energy Syst 2015;64:408–18.
- [16] Khaji M, Aghamohammadi MR. Emergency transmission line switching to suppress power system inter-area oscillation. Int J Electrical Power Energy Syst 2017;87:
- [17] Amraee T, Saberi H. Controlled islanding using transmission switching and load shedding for enhancing power grid resilience. Int J Electrical Power Energy Syst 2017;91:135–43.
- [18] Lin J, Hou Y, Zhu G, Luo S, Li P, Qin L, Wang L. Co-optimization of unit commitment and transmission switching with short-circuit current constraints. Int J Electrical Power Energy Syst 2019;110:309–17.
- [19] Li X, Balasubramanian P, Abdi-Khorsand M, Korad AS, Hedman KW. Effect of topology control on system reliability: TVA test case. In: In Proc. CIGREGrid Future Symp., Houston, TX, USA, Oct. 2014, p. 1–8.
- [20] Li X, Balasubramanian P, Sahraei-Ardakani M, Abdi-Khorsand M, Hedman KW, Podmore R. Real-time contingency analysis with corrective transmission switching. IEEE Trans Power Syst 2017;32(4):2604–17.
- [21] Sahraei-Ardakani M, Li X, Balasubramanian P, Hedman KW, Abdi-Khorsand M. Real-time contingency analysis with transmission switching on real power system data. IEEE Trans Power Syst 2016;31(3):2501–2.
- [22] Schnyder G, Glavitsch H. Security enhancement using an optimal switching power flow. IEEE Trans Power Syst May 1990;5(2):674–81.
- [23] Bacher R, Glavitsch H. Network topology optimization with security constraints. IEEE Trans Power Syst Nov 1986;1(4):103–11.
- [24] Mazi AA, Wollenberg BF, Hesse MH. Corrective control of power system flows by line and bus-bar switching. IEEE Trans Power Syst Aug 1986;1(3):258–64.
- [25] Wrubel JN, Rapcienski PS, Lee KL, Gisin BS, Woodzell GW. Practical experience with corrective switching algorithm for on-line applications. IEEE Trans Power Syst 1996;11(1):415–21.
- [26] Shao W, Vittal V. Corrective switching algorithm for relieving overloads and voltage violations. IEEE Trans Power Syst 2005;20(4):1877–85.
- [27] Goldis EA, Ruiz PA, Caramanis MC, Li X, Philbrick CR, Rudkevich AM. Shift factor-based SCOPF topology control MIP formulations with substation configurations. IEEE Trans Power Syst 2017;32(2):1179–90.

- [28] Heidarifar M, Doostizadeh M, Ghasemi H. Optimal transmission reconfiguration through line switching and bus splitting. In: 2014 IEEE PES General Meeting — Conference Exposition, July 2014, p. 1–5.
- [29] Xiang Y, Wang L, Xiao R, Xie K. Impact of network topology optimization on power system reliability. In: 2016 International Conference on Probabilistic Methods Applied to Power Systems (PMAPS), Oct 2016, p. 1–5.
- [30] Xiao R, Xiang Y, Wang L, Xie K. Power system reliability evaluation incorporating dynamic thermal rating and network topology optimization. IEEE Trans Power Syst 2018;33(6):6000–12.
- [31] Li Y, Xie K, Wang L, Xiang Y. Exploiting network topology optimization and demand side management to improve bulk power system resilience under windstorms. Electric Power Syst Res 2019;171:127–40.
- [32] Liu Z, Wang L. Leveraging network topology optimization to strengthen power grid resilience against cyber-physical attacks. IEEE Trans Smart Grid 2021;12(2): 1552-64
- [33] Li Y, Xie K, Wang L, Xiang Y. The impact of PHEVs charging and network topology optimization on bulk power system reliability. Electric Power Syst Res 2018;163: 85–97
- [34] Li Y, Hu B, Xie K, Wang L, Xiang Y, Xiao R, Kong D. Day-ahead scheduling of power system incorporating network topology optimization and dynamic thermal rating. IEEE Access 2019;7:35287–301.
- [35] Khanabadi M, Ghasemi H, Doostizadeh M. Optimal transmission switching considering voltage security and N-1 contingency analysis. IEEE Trans Power Syst Feb 2013;28(1):542–50.
- [36] Soroush M, Fuller JD. Accuracies of optimal transmission switching heuristics based on DCOPF and ACOPF. IEEE Trans Power Syst March 2014;29(2):924–32.
- [37] Capitanescu F, Wehenkel L. An AC OPF-based heuristic algorithm for optimal transmission switching. In: 2014 Power Systems Computation Conference, Aug 2014, p. 1–6.
- [38] Poyrazoglu G, Oh H. Optimal topology control with physical power flow constraints and N-1 contingency criterion. IEEE Trans Power Syst Nov 2015;30(6): 3063-71
- [39] Bai Y, Zhong H, Xia Q, Kang C. A two-level approach to AC optimal transmission switching with an accelerating technique. IEEE Trans Power Syst March 2017;32 (2):1616–25.
- [40] Kocuk B, Dey SS, Sun XA. New formulation and strong MISOCP relaxations for AC optimal transmission switching problem. IEEE Trans Power Syst Nov 2017;32(6): 4161–70
- [41] Park B, Demarco CL. Optimal network topology for node-breaker representations with AC power flow constraints. IEEE Access 2020;8:64347–55.
- [42] Hedman KW, O'Neill RP, Fisher EB, Oren SS. Optimal transmission switching with contingency analysis. IEEE Trans Power Syst 2009;24(3):1577–86.
- [43] Khodaei A, Shahidehpour M. Transmission switching in security-constrained unit commitment. IEEE Trans Power Syst 2010:25(4):1937–45.
- [44] Babaeinejadsarookolaee S, Birchfield A, Christie RD, Coffrin C, DeMarco C, Diao R, et al. The power grid library for benchmarking AC optimal power flow algorithms. arXiv preprint arXiv:1908.02788, 2019.
- [45] Low SH. Convex relaxation of optimal power flow part I: Formulations and equivalence. IEEE Trans Control Network Syst March 2014;1(1):15–27.
- [46] ISO-NE. ISO New England Planning Procedure No. 9, Major Substation Bus Arrangement Requirements and Guidelines. ISO New England, September 2017. https://www.iso-ne.com/static-assets/documents/rules_proceds/isone_plan/pp09/pp_9.pdf.
- [47] Williams HP. Model Building in Mathematical Programming. fifth ed. New York: Wiley; 2013.
- [48] University of Washington, Dept. of Electrical Engineering. Power Systems Test Case Archive. Published online at http://www.ee.washington.edu/research/pstca/, 1999. [Accessed: 19-Apr-2020].
- [49] Löfberg J. YALMIP: A toolbox for modeling and optimization in MATLAB. In: Proceedings of the CACSD Conference, Taipei, Taiwan; 2004.
- [50] Zimmerman RD, Murillo-Sanchez CE, Thomas RJ. MATPOWER: Steady-state operations, planning, and analysis tools for power systems research and education. IEEE Trans Power Syst 2011;26(1):12–9.